Plasma and Vacuum Carburizing Processes and Mechanical Properties of SCM 415 Steel

Dae-Wook Kim* and Byeong-Soo Lim**

(*Received February 18, 1999*)

The plasma and vacuum carburizing processes are innovative surface modification techniques for potential applications in manufacturing processes of vehicle components. In this study, the influence of this relatively new process on the surface hardness of SCM 415 low-alloy steel (0.15% C) was investigated under various process conditions involving gas composition, gas pressure, plasma current density, temperature and time. The effective plasma carburizing temperature of SCM 415 steel was found to be higher than 850℃, and the case depth was proportional to the square root of carburizing time under the same current density. Also, high cycle fatigue and dry wear characteristics of vacuum carburized SCM 415 steel were evaluated after various heat treatments. Comparing the fatigue and wear characteristics of vacuum carburized specimens to those of hot annealed or reheat quenched specimens, the wear resistant property as well as bending fatigue limits were found to be substantially improved. The optimum amount of retained austenite exists for the maximum fatigue strength in vacuum carburized steels. Through quantitative analysis of the retained austenite using X-ray diffractometer, this value was found to be about 4%.

Key Words: Plasma Carburizing, Vacuum Carburizing, Bending Fatigue Strength, Surface Modification, Dry Wear

1. Introduction

Vehicle components such as gears, crank shafts, clutch plates, cams, spindles, etc. should have enough toughness to endure fatigue or impact loads as well as high wear resistance. Usually, one of the methods for making materials with a tough core and hardened surface is surface modification. Carburizing is one of the representative techniques for surface modification, because it can provide thick and well-hardened layers more economically than other surface hardening methods like nitriding (Kim, et. al., 1990; Cavallaro, et. al., 1995; Krauss, 1990). At present, gas carburizing process, which is ineffective as well as pollutive, is widely applied in the industry. In order to solve the disadvantages of gas carburizing, innovative surface modification techniques such as vacuum carburizing and plasma carburizing have been developed (Choi and Byun, 1992; Schnatbaum and Melber, 1994; Conybear, et. al., 1992). The main reason for the improvement of fatigue strength in carburized steels is known to be due to high hardness and compressive residual stress. Also, factors such as microstructure, carbide formation, internal oxidation, microcracking and the amount of retained austenite are very important (Tobe, et. al., 1986; Kim and Kweon, 1996). According to prior studies, the reduction of retained austenite and grain size, achieved by reheat treatment, contribute to the improvement of fatigue strength in carburized steels (Kim and Kweon, 1996; Krauss, 1978). But Cavallaro (1995) showed that the reduction of retained austenite after sub-zero treatment decreases the fatigue strength. As for the wear characteristics,

* Graduate student, Dept. of Mech. Eng'g, University of Washington, Seattle, U. S. A.

** Professor, School of Mech. Eng'g, Sungkyunkwan University, chunchun-Dong, Jangan-Ku, Suwon, Korea

sub-zero treatment increases the wear resistance (Krauss, 1990; Carlson, et. al., 1991).

In this study, the influence of experimental variables and heat treatment in plasma and vacuum carburizing processes on mechanical properties is investigated for SCM 415 steel.

2. Experimental Procedures

2.1 Sample preparation

Table 1 shows the chemical composition of the hot drawn SCM 415 steel used in the study. For sample preparation, a commercialized vacuum carburizing unit and a specially designed plasma carburizing unit, whose main components include heat chamber, external heating system, vacuum system, cooling system, electronic control system, etc., were employed. In plasma carburizing, to remove the oxide layer and impurities on the specimen, plasma sputtering was performed prior to carburizing at 900℃ for 30 min. under the Ar and H_2 gas(1:1 ratio) with 400~450V plasma voltage and 23 mA/cm^2 current density.

Table 1 Chemical compostion.

element	C	Si	Mn	P	S	Ni	Cr	Mo	Cu	Fe
Wt. %	0.15	0.21	0.72	0.01	0.02	0.10	0.97	0.17	0.13	rem.

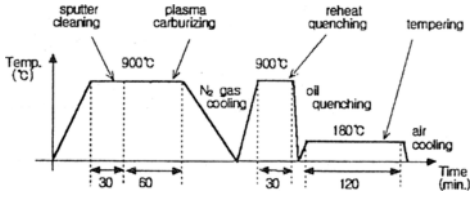

Fig. 1 Schematic diagram of plasma carburizing process.

The schematic diagrams of plasma and vacuum carburizing process are presented in Figs. 1 and 2. The specific heat treatment conditions for the 7 vacuum carburized specimens are shown in Table 2.

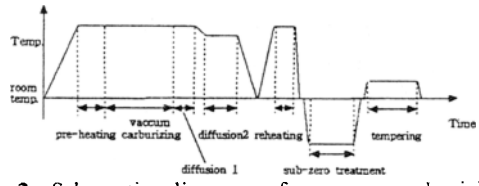

Fig. 2 Schematic diagram of vacuum carburizig process.

Table 2 Heat treatment conditions of vacuum carburized specimens.

No.	Temp.(℃) Time(min.)	Preheating	Vacuum carburizing	Diffusion 1	Diffusion 2	Reheating	Sub-zero treatment	Tempering
A	As-received							
B	Temp.	900	·	·	·	900	·	180
	Time	240	·	·	·	30	·	120
C	Temp.	900	900	900	810	·	·	180
	Time	50	350	50	30	·	·	120
D	Temp.	900	900	900	810	900	·	180
	Time	50	350	50	30	30	·	120
E	Temp.	900	900	900	810	900	−193	180
	Time	50	350	50	30	30	240	120
F	Temp.	900	900	900	830	900	·	180
	Time	60	450	60	60	30	·	120
G	Temp.	900	900	900	830	900	−193	180
	Time	60	450	60	60	30	240	120

2.2 Evaluation of mechanical properties

For the evaluation of mechanical properties, hardness, strength, rotation bending fatigue and dry wear tests were carried out. The surface hardness properties of both plasma and vacuum carburized specimens were investigated using microvickers hardness tester at 0.1mm intervals from the surface, using an indentation load of 200g.

The tensile properties were measured with 20 ton capacity hydraulic servo MTS and the fatigue properties were characterized by S-N curves obtained by JIS Z 2274 procedures at room temperature using Ono type rotation bending fatigue tester. The dry wear tests were conducted using a cylinder-on-disk type wear tester under 3kg load and at a constant speed of 110rpm (0.275m/s).

2.3 Observation of microstructure, fatigue fracture surface and measurement of the amount of retained austenite

The microstructure of surface layer and core were investigated using an optical microscope and the fracture surface due to fatigue failure was observed with a Scanning Electron Microscope (SEM). Auger Electron Spectroscopy (AES, Perkin-Elmer SAM 4300) was used to find out the change of carbon content after plasma carburizing. The electron beam current and voltage were set to 300nA and 5keV respectively. By line scanning and comparing the peak to peak height of the Auger spectrum, the relative carbon content was determined. The amount of retained austenite was measured by the X-ray diffraction method and an X-ray Diffractometer (XRD, MacScience, M18 XHF-SRA) was used. The intensities of the austenite peaks of {220} and {311} and ferrite peak of {211} were measured and the volume fractions were calculated (Miller, 1964).

3. Results

3.1 Surface hardening characteristics of plasma carburized specimens

Variables such as gas composition, gas pressure, plasma voltage, plasma current density, temperature and treatment time were employed in the plasma carburizing process to find out their effects on carburizing.

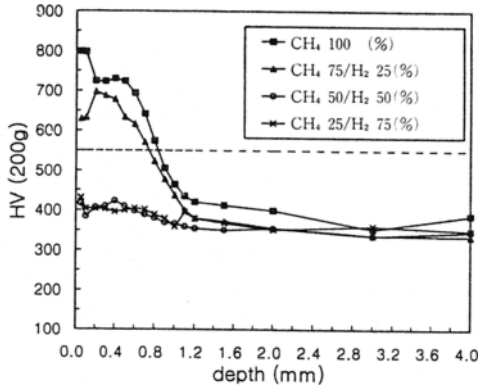

Fig. 3 The hardness profiles for various gas compositions. Dotted line for HV 550 represents the effective case depth. (Plasma carburized, reheat quenched, and tempered specimens)

To evaluate the effect of methane gas on SCM 415 steel in the plasma carburizing process, methane gas and hydrogen gas were mixed in different quantities. Fig. 3 shows the hardness profile for various gas compositions. Hydrogen gas was introduced because of its known effectiveness for some high Cr alloys to prevent oxidation and sooting during the carburization process and to improve the carburization uniformity. For 25% and 50% methane amounts, there was no carburizing effect. In Fig. 3 the effective case depth is defined as the layer depth greater than 550HV in hardness (SAE, 1964). When the methane gas amounted to over 75%, an effective case depth was achieved and with 100% methane gas, the maximum effective case depth was obtained. This result shows that the effective case depth depends on the amount of methane gas for plasma carburizing.

To find the effect of process pressure, pressure was controlled from 2 to 10 torr. Figure 4 shows that the carburizing effect became greater as the process pressure increased and, therefore, deep effective case depth was obtained. It should be noted that high process gas pressure caused the current density to increase at the same voltage and that the plasma intensity became stronger, which caused the carbon diffusion to the core to increase.

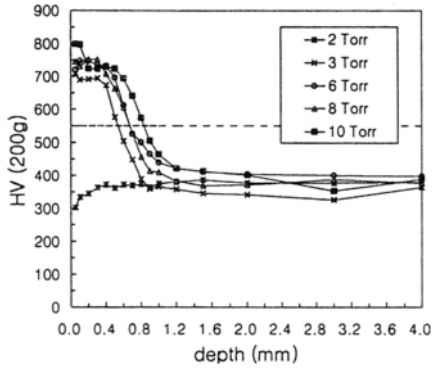

Fig. 4 The hardness profiles for various gas pressure conditions. (Plasma carburized, reheat quenched, and tempered specimens)

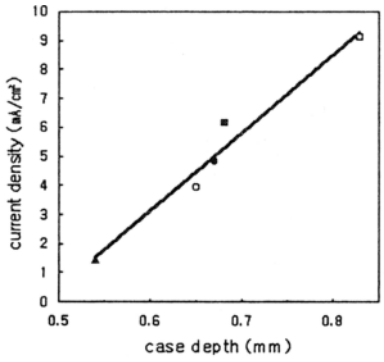

	Pressure during plasma carburizing (Torr)	Plasma voltage (V)
□	10	488
■	8	510
●	6	447
○	8	428
▲	3	517

Fig. 5 Relationship between current density and case depth. (Plasma carburized, reheat quenched, and tempered specimens)

Also in the case of same gas pressure, the change in the current density caused by the change of plasma voltage was found to have the same influence on the carburizing effect.

The current density and the effective case depth are proportional regardless of the gas pressure or plasma voltage as shown in Fig. 5. This is believed to be the effect of the increased carbon content on the surface due to the increased current density. To prove this, the variation of carbon

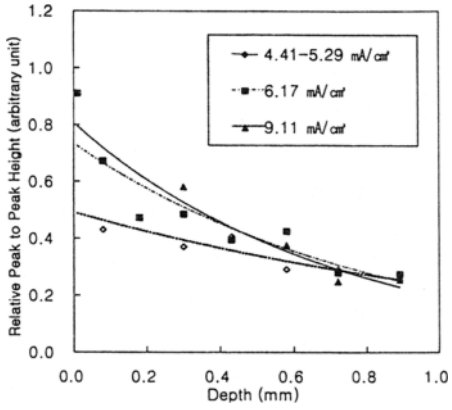

Fig. 6 Variation of relative carbon content with the current density.

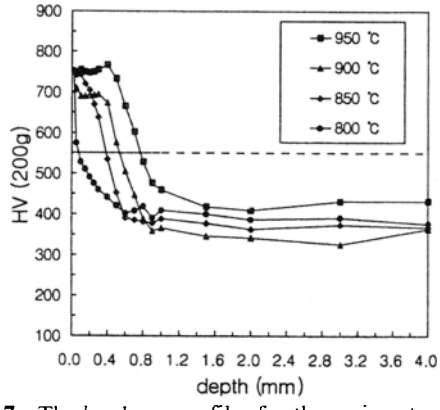

Fig. 7 The hardness profiles for the various temperatures. (Plasma carburized, reheat quenched, and tempered specimens)

content against the current density was investigated with AES. As shown in Fig. 6, the high current density caused the high carbon content at the same depth.

Figure 7 shows the effect of temperature on the carburized steel hardness in plasma carburizing. Below 800℃, an effective case depth was hardly obtainable, because of low carbon solubility in α iron. However, above 850℃, which is the austenizing temperature for plain carbon steel of 0.15%, a remarkable carburizing effect was noted, which became greater as the temperature increased. The effective case depth increased proportionally with the square root of carburizing time. Also, at 900℃, with the current density of 8.96~9.11mA/cm², the growth rate was calculated to be 0.017

mm/sec$^{1/2}$. The mechanical properties other than surface hardness characteristics are reported elsewhere in detail by the authors (Kim, et. al., 1998).

3.2 Mechanical properties of vacuum carburized specimens

The effective case depth and the hardness values from the surface down to the depth of 500μm of the vacuum carburized specimens are shown in Table 3. Compared with the non sub-zero treated specimens, the sub-zero treated specimens resulted in the hardness increase of about 50HV. As for the microstructure, specimen A had the typical annealed structure of mixture of ferrite and pearlite, while specimen B showed bainite structure which was also observed in the core of the carburized specimens. Specimen C had the tempered martensite structure with retained austenite, which decreased in specimen D. Sub-zero treatment did not alter the microstructure much, but it decreased the amount of the retained austenite. Fig. 8 shows the typical microstructures of specimen A, C and E.

Table 3 also shows the tensile and fatigue properties of each specimen. Under the tensile load, the non-carburized specimens (A, B) failed after yielding, while the carburized ones (C, F) with higher tensile strength property, failed with little plastic deformation and without yielding phenomena. From the effective case depth and tensile data as shown in Table 3, it can be seen that under the same heat treatment conditions, as the case depth increases the tensile stress increases. For example, as shown in the data for D and F, increasing the case depth from 0. 9mm to 1. 1mm resulted in 12% increase in the tensile stress.

Figure 9 shows the S-N diagrams of non-carburized (A, B), only carburized (C), and reheat treated after carburization (D, F) specimens. Comparing the data of A and B, the reheat treat-

Table 3 Effective case depth, surface hardness, ultimate tensile stress and fatigue strength of vacuum carburized specimens.

Specimen No.	Effective Case Depth (mm)	Surface Hardness (HV, 200g)	Ultimate Tensile Stress (MPa)	Fatigue Strength (MPa)
A	-	170~220	527	220
B	-	350~440	760	380
C	0.9	630~695	1230	600
D	0.9	676~712	1326	690
E	0.9	706~762	1338	620
F	1.1	670~715	1491	680
G	1.1	712~762	1407	500

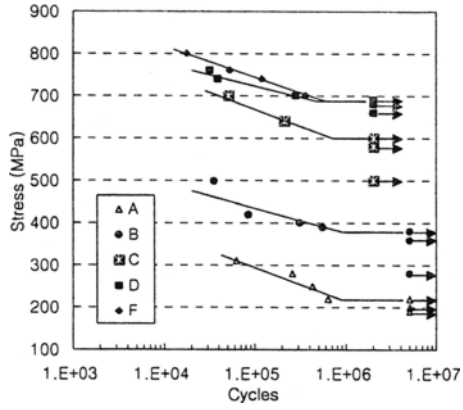

Fig. 9 S-N diagrams for specimens A, B, C, D and F.

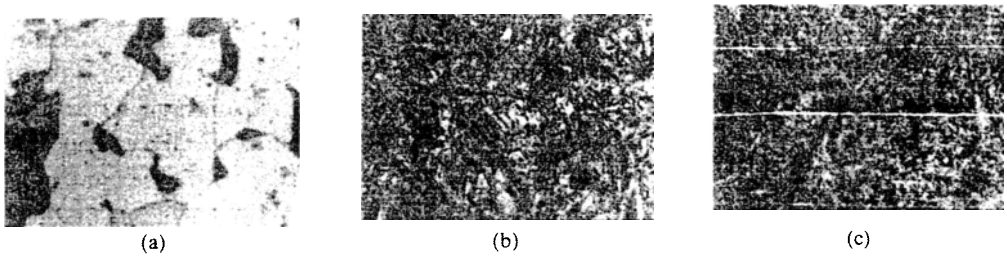

(a) (b) (c)

Fig. 8 Typical microstructures at 200 μm from the surface, $\times$1000; (a) Specimen A, (b) Specimen C and (c) Specimen E.

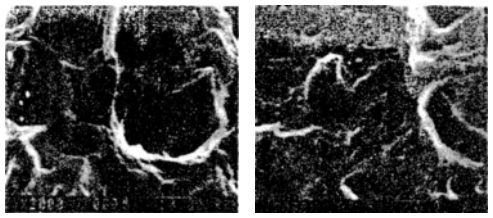

(a) (b)

Fig. 10 SEM micrographs of fatigue fracture surface of specimens (×2000), (a) Direct-quenched specimen C, (b) Reheat-quenched specimen D.

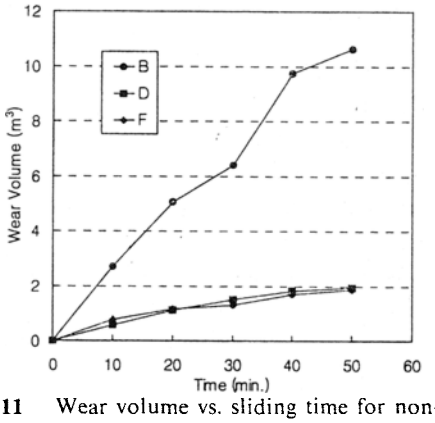

Fig. 11 Wear volume vs. sliding time for non-carburized specimen B and carburized specimens D, F.

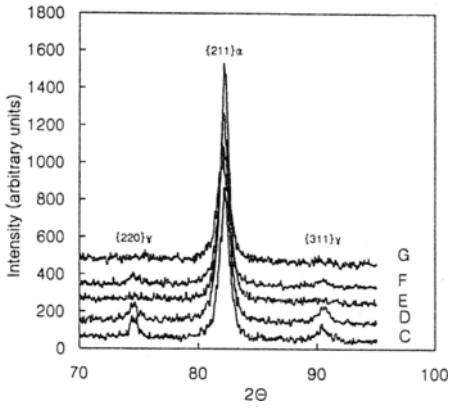

Fig. 12 Diffractometer trace for each specimen.

Table 4 Volume fraction of retained austenite for each specimen.

Specimen No.	Heat treatment condition	Retained austenite vol. fraction (%)
C	direct quenched	12
D	reheat quenched	4.2
E	reheat quenched and sub-zero treated	1.5
F	reheat quenched	5.5
G	reheat quenched and sub-zero treated	1.8

ment increased the fatigue strength by about 70% from 220 to 380MPa. Vacuum carburization improved the fatigue strength remarkably, as in the case of C whose fatigue strength increased to 600MPa compared with 380MPa of specimen B, the non-carburized one, which corresponds to about 58% increase. Also, the reheat treatment improved the fatigue strength by about 15% as is the case for specimens D and C. This result agrees with the prior reports (Kim and Kweon, 1996; Krauss, 1978) which showed that the decrease in both grain size and the amount of retained austenite increases the fatigue strength. The SEM observation of the fracture surface of specimens C and D revealed the clear difference in the fracture mode caused by reheat treatment. As Fig. 10 shows, the fracture surface of C (without reheat treatment) exhibits only the intergranular fracture aspects, while the reheated specimen, D, shows the mixture of inter and transgranular fracture features.

The carburization improved not only fatigue strength but also the wear resistance property due to the hardness increase. Figure 11 shows the reduction of wear volume for the carburized specimens (D, F) by about 5 times compared with the non carburized specimen, B.

Sub-zero treated specimens increased in surface hardness compared with non sub-zero treated ones. This is believed to be the result of the retained austenite transformation into martensite, which existed in the surface of the carburized specimen. To confirm this, the volume change of retained austenite was measured with XRD.

Fig. 12 indicates the variation of α and γ peak intensities of each specimen. From the peak intensity, the volume fraction of retained austenite was calculated using the Miller's equation (Miller,

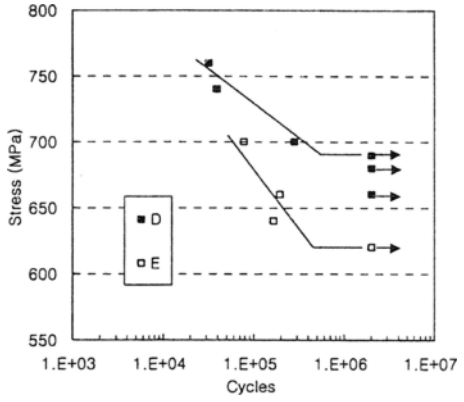

Fig. 13 S-N diagrams for specimens D and E.

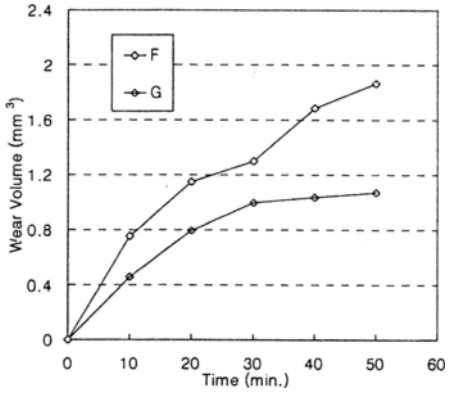

Fig. 14 Wear volume vs. sliding time for non sub-zero treated specimen F and sub-zero treated specimen G.

1964) and the results are presented in Table 4. As can be seen in Fig. 11, the sub-zero treated specimens (E, G) did not show any significant peaks of {220} or {311}, which means that most of the retained austenite transformed into martensite by sub-zero treatment. From the data of C, D and F in Table 4, it can be seen that the reheat treatment reduces the amount of retained austenite significantly.

Fig. 13 shows the S-N diagrams of non sub-zero treated specimen D and sub-zero treated specimen E. From the figure, it can be seen that the sub-zero treatment decreases the fatigue strength by 50MPa, which is about 11%, due to the reduction of the amount of retained austenite.

To investigate the change in the wear property by sub-zero treatment, the wear volume-time

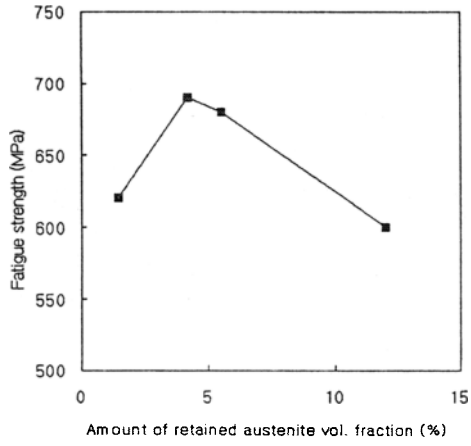

Fig. 15 Influence of the amount of retained austenite on the fatigue strength.

diagram was constructed as shown in Fig. 14. With the same case depth, the sub-zero treated specimen, G, showed improved wear resistance compared with the non sub-zero treated specimen, F. This is believed to be the result of greater martensite content in specimen G.

Figure 15 shows the change of fatigue strength against the amount of retained austenite. From the figure, it seems that there exists some specific volume of retained austenite, which is around 4%, where optimum fatigue strength can be obtained. Similar results were reported in previous studies as well (Cavallaro, 1995; Prado, 1984).

4. Conclusions

From the experimental results, the following conclusions can be made for SCM 415 steel in plasma carburizing and vacuum carburizing processes.

(1) The effective case depth was found to be dependent on the amount of methane gas in the plasma carburizing process. The deepest case depth and uniform hardness was obtained with 100% methane gas.

(2) The case depth increased with the plasma current density. Higher current density caused more diffusion of carbon, resulting in greater effective case depth.

(3) The effective plasma carburizing tempera-

ture of SCM 415 steel was found to be higher than 850℃, and the case depth incrcases with temperature.

(4) In vacuum carburizing process, the reheat treated specimens were found to be superior to the direct quenched specimens in tensile strength and fatigue strength. Also, the increase in effective case depth increases the tensile strength as well as the fatigue strength. As for the mode of failure surface, both transgranular as well as intergranular fracture modes were observed in the reheat treated specimens.

(5) Sub-zero treatment had a negative influence on the bending fatigue properties, and only the intergranular fracture aspects were observed on the surface of sub-zero treated specimens which failed by fatigue.

(6) Surface hardness improved by carburizing resulted in better wear resistance. Also, wear resistance of sub-zero treated specimen was higher than that of non sub-zero treated specimens. This resulted from the increase of hardness by the martensite transformation of more retained austenite.

(7) At about 4% of retained austenite, maximum fatigue strength was obtained within the scope of this experiment.

Acknowledgement

This research was supported by Safety & Structural Integrity Research Center (SAFE), Sungkyunkwan University.

References

Carlson, E. A., Cold Treating and Cryogenic Treatm Juvinall, C. R., 1991, *Fundamentals of Machine Component Design*, 2nd Ed. John Wiley & Sons, pp. 81~96.

Cavallaro, G. P., 1995, "Bending Fatigue and Contact Fatigue Characteristics of Carburized Gears," *Surface & Coating Technology* 71, pp. 182~192.

Choi, Y. T., Byun, S. K., 1992, *J. the Korean Society for Heat Treatment* Vol. 5, No. 1, pp. 32~40.

Conybear, J. G., et. al., 1992 "Plasma Carburize High Alloy Bearing, Gear Steels," *Heat Treating*, pp. 11~13.

Evanson, K., Krauss, G., and Medlin, D., 1995, "Bending Fatigue Behavior of Vaccum Carburized AISI 8620 Steel", *Proceedings of the 2nd International Conference on Carburizing and Nitriding with Atmospheres,* 6-8 December 1995, Cleveland, Ohio. ASM International, pp. 61~69.

Kim, D. W., Kim, D., Lim, B. S and Kim, S. B., 1998, "Characteristics of Plasma Carburizing Process in Surface Hardening of SCM415 steel," *Korean T. of Materials Research*, Vol. 8, No. 8, pp. 707~713.

Kim, H. J. and Kweon, Y. G., 1996, "High Cycle Fatigue Behavior of Gas-Carburized Medium Carbon Cr-Mo Steel," *Meta. Trans. A*, Vol. 27A, pp. 2557~2564.

Kim, H. K, Kim, K. S., Kil, S. C., 1990, "New Heat Treatment Technique," *KIET*, pp. 189~191.

Krauss, G., 1978, "The Microstructure and Fracture of a Carburized Steel," *Meta. Trans.* A, Vol. 9A, pp. 1527~1535.

Miller, R. L., 1964, "A Rapid X-Ray Method for the Determination of Retained Austenite," *Transactions of ASM*, Vol. 57, pp. 892~899.

Prado, J. M., 1984, "Influence of Retained Austenite on the Fatigue Endurance of Carbonitrided Steels," *J. Mater. Sci.*, Vol. 19, pp. 2980~2988.

SAE, 1964, *Methods of Measuring Case Depth*, Metals Handbook 8th Ed. Vol. 2., pp. 164~165.

Schnatbaum, F. and Melber, A., 1994, "Plasma Carburizing of Steel in Pulsed Direct-Current Glow Discharges," *Heat Treatment of Metals*, pp. 45~51.

Tobe, *et. al.*, 1986, "Bending Strength of Carburized SCM420H Spur Gear Teeth," *Bulletin of JSME*, Vol. 29, pp. 273~280.